

# New interactions in the dark sector mediated by dark energy

Anthony W. Brookfield,<sup>1,2,\*</sup> Carsten van de Bruck,<sup>1,†</sup> and Lisa M.H. Hall<sup>1,‡</sup>

<sup>1</sup>*Astroparticle Theory and Cosmology Group, Department of Applied Mathematics,  
The University of Sheffield, Hounsfield Road, Sheffield S3 7RH, United Kingdom*

<sup>2</sup>*Astroparticle Theory and Cosmology Group, Department of Physics and Astronomy,  
The University of Sheffield, Hounsfield Road, Sheffield S3 7RH, United Kingdom*

Cosmological observations have revealed the existence of a dark matter sector, which is commonly assumed to be made up of one particle species only. However, this sector might be more complicated than we currently believe: there might be more than one dark matter species (for example two components of cold dark matter or a mixture of hot and cold dark matter) and there may be new interactions between these particles. In this paper we study the possibility of multiple dark matter species and interactions mediated by a dark energy field. We study both the background and the perturbation evolution in these scenarios. We find that the background evolution of a system of multiple dark matter particles (with constant couplings) mimics a single fluid with a time-varying coupling parameter. However, this is no longer true on the perturbative level. We study the case of attractive and repulsive forces as well as a mixture of cold and hot dark matter particles.

## I. INTRODUCTION

Cosmological observations of the largest structures in the universe, the anisotropies in the cosmic microwave background (CMB) radiation and Type Ia supernovae suggest that normal matter contributes only 4% of the total energy budget of the universe [1, 2, 3]. The majority of energy and matter is made up of cold dark matter (CDM, 21%), which clusters on scales of galaxies and clusters of galaxies, and a much more homogeneous distributed dark energy component (75%). Whereas dark matter candidates are well motivated within particle theories beyond the standard model, it is fair to say that the discovery of the accelerated expansion of the universe came as a surprise and that it will be much harder to interpret within particle physics theories. Candidates for dark energy include the cosmological constant (e.g. [4]), scalar fields (see e.g. [5, 6, 7, 8, 9, 10, 11, 12, 13, 14, 15, 16, 17, 18, 19, 20, 21]) or vector fields (see e.g. [22, 23, 24]). When analysing the data it is usually assumed that General Relativity is the correct theory of gravity at the largest visible scales. Of course, dark energy might signal a breakdown of General Relativity itself, a possibility which has been recently studied in detail (see e.g. [25, 26, 27, 28, 29, 30, 31, 32, 33, 34, 35, 36, 37, 38, 39, 40, 41] and references therein for recent work). In this paper, however, we will assume that dark energy can be attributed to a slow-rolling scalar field, interacting with other matter forms present in the universe, most notably with CDM and hot dark matter (HDM, in the form of massive neutrinos for example).

Since the nature of dark energy remains unknown, it is important to study new effects resulting from dark energy and its possible interactions with the rest of the world.

Whereas new forces between normal matter particles are heavily constrained by observations (e.g. in the solar system and gravitational experiments on Earth), this is not the case for neutrinos and dark matter particles. At the moment, constraints on new forces between neutrinos or dark matter can only come from cosmological observations. Additionally, it is usually assumed that there is only one type of dark matter; this is well motivated by supersymmetrical models which predict that dark matter is the lightest supersymmetric particle. However, there might be more than one dark matter species. Such a possibility has been investigated previously in [19] and can be motivated from string theory [42, 43]. In this paper, we study the cosmological implications of a dark sector with multiple matter species (CDM, HDM) and consider the possibility that new forces are mediated between the particles by a dark energy scalar field. The aim is to study both the background evolution as well as the evolution of perturbations in the CDM and/or HDM fluids. We take into account the full evolution of the HDM component, both for the background as well as on the perturbative level [44, 45]. We will see that there are new effects associated with new forces in the CDM and/or HDM sector, and there is much hope that cosmological data will strongly constrain such interactions. We do not address the question of whether the effects of the new interactions are inherent in alternative theories of gravity, a possibility which has been pointed out before [46]. In both coupled quintessence (including models considered here) and modified gravity, the growth rate of density fluctuations will be modified due to the presence of new degrees of freedom. This may lead to a degeneracy between these models when only linear perturbations are taken into account.

The new force mediated by the dark energy scalar field is always attractive for particles of the same kind. However, if the couplings for the individual species (to be defined in the next section) have opposite signs, the force between different forms of matter will be repulsive. For the cases studied in this paper the force mediated by dark

---

\*Email address: php04awb@sheffield.ac.uk

†Email address: C.vandeBruck@sheffield.ac.uk

‡Email address: Lisa.Hall@sheffield.ac.uk

energy is always long-ranged. As a result, the total force acting on the dark sector particles (i.e. the sum of the gravitational force and the new force) can be smaller than the gravitational force itself or even repulsive, depending on the coupling. In addition, we will see that when the couplings have opposite signs, the expansion of the universe in the matter dominated era can behave as if there is no new interaction between the particles. Cosmological structure formation, however, is affected by the presence of the new forces.

When studying concrete examples, we will assume that there are only two dark species and one dark energy scalar field. The paper is organized as follows. In the next Section, we describe the background evolution for three typical models. In Section 3, we study the perturbations in these models, calculating both CMB anisotropy and matter power spectra. We conclude in Section 4.

## II. BACKGROUND EVOLUTION

We consider a system of  $N$  species of matter coupled to a single scalar field  $\phi$ , which we assume will be responsible for the late-time accelerated expansion of the universe. We assume a flat, homogeneous Friedmann-Robertson-Walker universe with line-element given by

$$ds^2 = a(\tau)^2 (-d\tau^2 + \delta_{ij} dx^i dx^j). \quad (1)$$

The Einstein equations, describing the evolution of the scale factor  $a(\tau)$ , are given by

$$H^2 \equiv \left(\frac{\dot{a}}{a}\right)^2 = \frac{8\pi G a^2}{3} \rho, \quad (2)$$

$$\dot{H} = -\frac{4\pi G a^2}{3} (\rho + 3p), \quad (3)$$

where  $\rho(\tau)$  and  $p(\tau)$  are the total energy density and pressure respectively, and overdots represent differentiation with respect to conformal time  $\tau$ . In the following we set  $8\pi G = 1$ .

As is customary, we define  $\beta_i$  as the strength of the coupling between the  $i^{\text{th}}$  matter species and the scalar field, which is given by

$$\beta_i \equiv \frac{d \ln m_i(\phi)}{d\phi}, \quad (4)$$

where  $m_i$  is the particle mass of species  $i$ . Conservation of energy momentum for each of the coupled fluids requires that

$$T_{\gamma;\mu}^\mu = \beta \phi_{,\gamma} T_\alpha^\alpha \quad (5)$$

which yields

$$\dot{\rho}_i + 3H(\rho_i + p_i) = \beta_i \dot{\phi} (\rho_i - 3p_i) \quad (6)$$

in the Robertson-Walker spacetime for each of the individual coupled matter species. The evolution of the

scalar field is described by the Klein-Gordon equation, which in the presence of matter couplings is given by

$$\ddot{\phi} + 2H\dot{\phi} + a^2 \frac{dV}{d\phi} = -a^2 \sum_{i=1}^N \beta_i (\rho_i - 3p_i). \quad (7)$$

In order to investigate the late-time attractor solutions of this system, we perform the usual transformation of variables

$$\begin{aligned} x &= \frac{\dot{\phi}}{H\sqrt{6}}, & y &= \frac{1}{H} \sqrt{\frac{V}{3}} \\ z &= \frac{1}{H} \sqrt{\frac{\rho_\gamma}{3}}, & u_i &= \frac{1}{H} \sqrt{\frac{\rho_i}{3}} \\ v &= \frac{1}{H} \sqrt{\frac{\rho_b}{3}}, \end{aligned}$$

with

$$x^2 + y^2 + z^2 + \sum_{i=1}^N u_i^2 + v^2 = 1. \quad (8)$$

In these equations,  $\rho_\gamma$  and  $\rho_b$  are the energy density of radiation and baryons respectively. Note that in the following we assume that  $\beta_i$  is constant and  $u_i$  is non-relativistic (which is valid for late times). We also use the Friedmann constraint (Eqn. (8)) to eliminate  $v$  and consider a general quintessence potential with

$$\lambda \equiv -\frac{1}{V} \frac{dV}{d\phi}. \quad (9)$$

Differentiation with respect to  $\alpha = \ln a$  yields the following set of equations,

$$H' = -\frac{3}{2}H \left[ 1 + x^2 - y^2 + \frac{1}{3}z^2 \right] \quad (10)$$

$$x' = \sqrt{\frac{3}{2}}\lambda y^2 - \sum_{i=1}^N \sqrt{\frac{3}{2}}\beta_i u_i^2 - x \left( 3 + \frac{H'}{H} \right) \quad (11)$$

$$y' = -\sqrt{\frac{3}{2}}\lambda xy - y \frac{H'}{H} \quad (12)$$

$$z' = -z \left( 2 + \frac{H'}{H} \right) \quad (13)$$

$$u_i' = \sqrt{\frac{3}{2}}\beta_i u_i x - u_i \left( \frac{3}{2} + \frac{H'}{H} \right). \quad (14)$$

It has been shown in [16] that for a single coupled fluid with an exponential coupling and exponential potential there are two late time attractor solutions consistent with an accelerating universe. The critical point for the first solution (Attractor A) is characterised by  $\Omega_\phi = 1$  at late times, and leads to acceleration provided  $\lambda < \sqrt{2}$ . The second critical point (Attractor B) is a scaling solution, with  $\Omega_\phi$  dependent upon the choice of  $\beta$  and  $\lambda$ . This solution results in acceleration if  $\lambda < 2\beta$ . For full details we refer to [16].

Case	$\lambda$	Species		Coupling		Relative Densities $\left(\frac{\Omega_1}{\Omega_2}\right)_0$
		1	2	$\beta_1$	$\beta_2$	
I	$\sqrt{\frac{3}{2}}$	CDM	CDM	4.0	0.1	$5.2 \times 10^{-4}$
II	$\sqrt{\frac{3}{2}}$	CDM	CDM	-1.5	1	0.28
III	2	HDM	CDM	5.8	-0.1	0.56

TABLE I: Cases considered in this paper: Two cases (I, II) with two species of CDM and one case (III) with CDM and HDM. For all cases  $\phi_{\text{initial}} = 0.1$  and we consider a flat universe with cosmological parameters:  $h = 0.7$ ,  $\Omega_b^{(0)} h^2 = 0.022$  and  $\Omega_{\text{CDM}}^{(0)} h^2 = 0.12$  for the coupled CDM species.

We find that introducing multiple coupled fluids does not affect this result because at late times the system reduces to the single fluid case as the highly coupled fluids dilute at a faster rate. Indeed, the only non-trivial additional critical point which arises due to the addition of multiple coupled species is characterised by

$$\sum_{i=1}^N \beta_i u_i^2 = 0, \quad (15)$$

with  $x = y = z = 0$  and  $\Omega_\phi = 0$ . This solution does not lead to an accelerating cosmology, but can play an important role as a transient solution during the matter dominated epoch, as we will discuss later.

In order to obtain an understanding of the background evolution, it turns out to be useful to combine the coupled matter species into a single effective fluid, with total energy and pressure given by

$$\rho_c = \sum_{i=1}^N \rho_i, \quad p_c = \sum_{i=1}^N p_i, \quad (16)$$

and an effective coupling  $\beta_{\text{eff}}$  given by

$$\beta_{\text{eff}} \equiv \frac{\sum_{i=1}^N \beta_i (\rho_i - 3p_i)}{\rho_c - 3p_c}. \quad (17)$$

We can therefore recast our multi-fluid system of conservation equations into a single conservation equation for  $\rho_c$  with an effective coupling  $\beta_{\text{eff}}$ . We will see later that this is only possible for the background. It should be further noted that the effective coupling is a function of both the scalar field and the energy densities of the coupled fluids, and therefore will in general vary in time even if the couplings of the individual fluids are constant. In other words, an observer, studying the background evolution and assuming a single fluid only, will deduce that the coupling evolves in time, although there are several species with constant individual couplings.

We now consider the effect on the cosmological background of coupling multiple fluids to the scalar field. For simplicity, we assume that there are two species of coupled matter, and that the form of the coupling between

the coupled fluids and the scalar field is of exponential form for concreteness:

$$m_i(\phi) = m_i^{(*)} e^{\beta_i \phi}. \quad (18)$$

We also take a typical quintessence exponential potential for the scalar field, namely

$$V(\phi) = M e^{-\lambda \phi}, \quad (19)$$

where  $M$  and  $\lambda$  are chosen to give late time acceleration today.

It is instructive to consider three cases, each distinguished by either the sign of the coupling or the type of dark matter considered. The specifications can be found in Table I. In the first two cases (I,II) we consider two types of CDM, but while the individual couplings  $\beta_1$  and  $\beta_2$  are both positive in Case I, the couplings have opposite signs in Case II. For both of these cases we choose  $\lambda$  and  $\beta_i$  such that the system approaches the accelerated late-time attractor with  $\Omega_\phi = 1$  (Attractor A). A scenario with mass-varying neutrinos (as a single coupled species) in which the system approaches Attractor A has been studied in [21, 44]. As will be apparent later, the chosen parameters lead to a consistent background cosmology but the predicted matter power spectra differ significantly from the  $\Lambda$ CDM case and are observationally ruled out. The purpose of this paper, however, is to illuminate the physical effects of these models and the extreme parameter choices reflect this.

It is possible to consider a scenario in which a system with two CDM species reaches the late-time accelerated scaling solution (Attractor B). In order to achieve an observationally consistent cosmology, this would require one species to remain sub-dominant until today, when it would begin to scale with dark energy. In this case, the mass of such a species would vary greatly, most likely leading it to become relativistic in the past. This is the third scenario we consider (Case III), in which a dominant CDM component and a subdominant HDM component each couple to dark energy.

A similar system, albeit with the CDM uncoupled to dark energy, has recently been considered in [47] in the context of neutrinos with a growing mass. We choose  $\lambda$  smaller than in this latter paper. Additionally, we choose to take couplings with opposite signs, such that the mass of the HDM particle grows in time. Note that for the HDM species, we fully consider both the non-relativistic and relativistic behaviour of the particles, integrating the Fermi-Dirac distribution function over phase space [48].

In Cases I & II the particles are highly non-relativistic. Then, from eqn. (6) and using  $p_i = 0$ , the evolution of the energy density of the  $i^{\text{th}}$  coupled fluid is given by

$$\rho_i = \frac{\rho_i^{(*)} e^{\beta_i \phi}}{a^3} = \frac{\rho_i^{(0)} e^{\beta_i (\phi - \phi_0)}}{a^3}, \quad (20)$$

where  $\rho_i^{(0)}$  is the energy density of species  $i$  at the present epoch. With this choice of couplings and two CDM

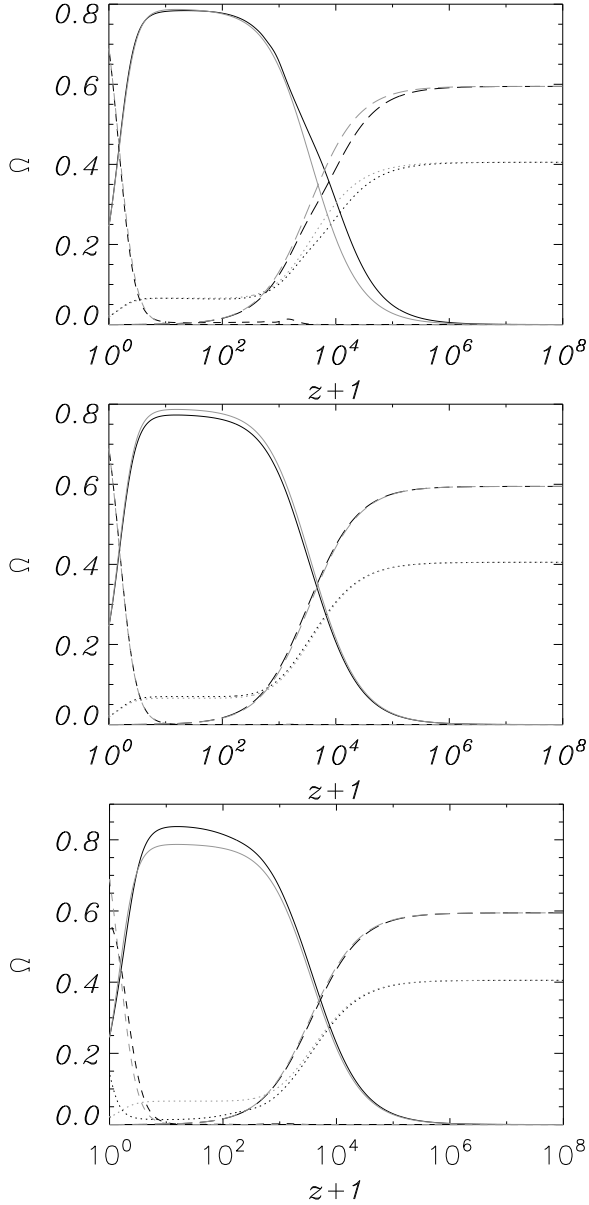


FIG. 1: Relative energy densities for Case I, II and III. Solid line: Coupled CDM. Long-dashed line: radiation. Short-dashed line: dark energy. Dotted line: neutrinos. The faint curves show a typical cosmology with  $\beta = 0$  for comparison.

species, an observer assuming a single fluid would detect a time-dependent coupling, which would take the form:

$$\beta_{\text{eff}}(\phi) = \frac{Ae^{B\phi} + C}{1 + A} \quad (21)$$

where  $A = \beta_1 \rho_1^{(*)} / \rho_2^{(*)}$ ,  $B = \beta_1 - \beta_2$ ,  $C = \beta_2$  and are all constant.

The evolution of the density parameters are shown in Fig. 1 for the three cases. The effective coupling experienced by the combined fluid, as defined in eq. (17), is the weighted value of the coupling strengths of the two fluids,

where the weighting factor is given by  $(\rho_i - 3p_i)$ . Hence, if the fluid with larger coupling (e.g. species 2 with  $\beta_2$ ) is dominant at early times, then  $\beta_1 \leq \beta_{\text{eff}} \leq \beta_2$ . However, the species with the higher value of coupling also dilutes at a greater rate, and so at later times this species becomes sub-dominant, and the effective coupling tends towards the lower value for  $\beta$ . The evolution of  $\beta_{\text{eff}}$  is shown in the left panel of Fig. 2.

The effect of the couplings on the background evolution is to modify the evolution of the energy densities of the coupled fluids. Therefore, even if the density parameters are tuned to the standard values today (i.e.  $\Omega_\phi \approx 0.7$ ,  $\Omega_{\text{CDM}} \approx 0.25$ ), their values at early times are different from what one would expect in the uncoupled case. This will affect, among other things, the predictions for the CMB anisotropies.

As can be seen in Fig. 2, for Case II, the effect of choosing opposite signs for  $\beta$  for the two fluids is to drive the effective coupling of the combined fluid towards zero during the matter dominated epoch. Therefore for some period of time the background cosmology of the system behaves essentially identical to the usual uncoupled case. We can best understand this behavior by considering a transient solution to Eqns (10-14) which is valid when the coupled matter species dominates the energy density. In this regime we can take  $u'_i = 0$  and  $x^2, y^2, z^2 \ll u_i^2$  and  $x', y', z' \sim 0$ , which leads to a critical point given by Eqn (15), which is equivalent to  $\beta_{\text{eff}} = 0$ . This transient regime ends when the energy density stored in the scalar field becomes non-negligible.

More heuristically, if we instead consider the dynamics of the scalar field, then the evolution of  $\phi$  is driven by the properties of the effective potential

$$\frac{dV_{\text{eff}}}{d\phi} \equiv \frac{dV}{d\phi} + \sum_{i=1}^N \beta_i \rho_i, \quad (22)$$

which during the matter dominated epoch can be approximated by

$$\frac{dV_{\text{eff}}}{d\phi} \approx \sum_{i=1}^N \beta_i \rho_i, \quad (23)$$

if the potential can be neglected, which is usually the case for quintessence potentials and in models where the couplings are of opposite signs. Clearly, in this scenario, the effective potential will have a minimum located at

$$\phi_{\text{min}} = \frac{1}{\beta_1 - \beta_2} \ln \left( \frac{-\beta_2 \rho_2^{(*)}}{\beta_1 \rho_1^{(*)}} \right). \quad (24)$$

We can expect the field to sit in this minimum if  $m_\phi^2 \equiv \frac{d^2 V_{\text{eff}}}{d\phi^2} > (H/a)^2$ , i.e.

$$\left( \frac{H}{a} \right)^2 \approx \frac{1}{3} (\rho_1 + \rho_2) < \beta_1^2 \rho_1 + \beta_2^2 \rho_2, \quad (25)$$

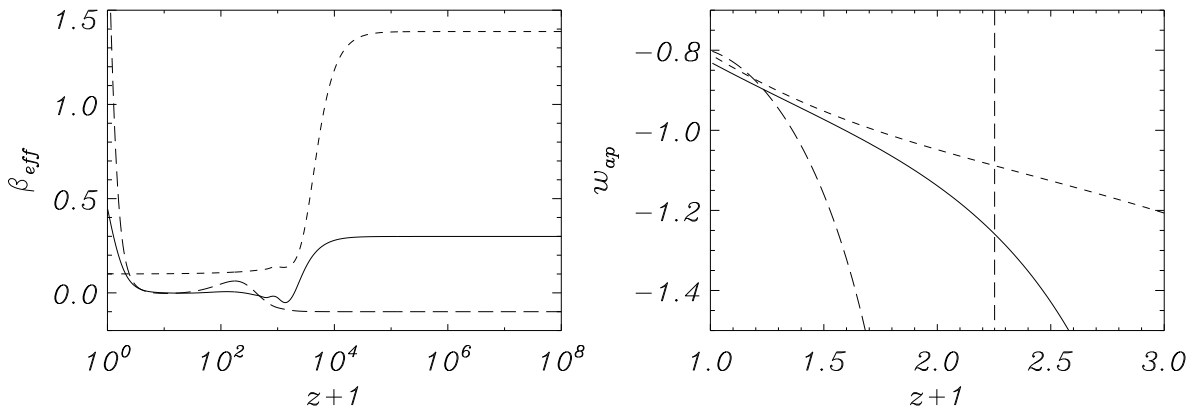


FIG. 2:  $\beta_{\text{eff}}$  and  $w_{\text{ap}}$  for the three cases. Short-dashed line: Case I. Solid line: Case II. Long-Dashed line: Case III. Note that for Case III,  $x$  (as defined in Eqn. (29)) goes through unity when  $z \sim 1.2$  and  $w_{\text{ap}}$  becomes undefined.

which requires

$$(\beta_1 - \beta_2)(\beta_1\beta_2 + 1/3) > 0 \quad (\text{assuming } \beta_2 > 0) \quad (26)$$

and hence  $\beta_2 > -\frac{1}{3\beta_1}$ . Therefore, provided this constraint is satisfied, and  $\beta_1$  and  $\beta_2$  are of opposite sign, we can expect  $\beta_{\text{eff}}$  to be driven to zero during the matter dominated epoch as the field will be forced to sit in the minimum of the effective potential. Note in particular that this behavior is independent of the *form* of  $V$ , provided that the scalar field satisfies the conditions discussed above. When this condition is not satisfied the evolution of the system resembles that of Case I.

Case III is unlike the previous two cases in that the values of  $\lambda$  and  $\beta$  are chosen such that the system approaches the accelerated scaling attractor (Attractor B). This requirement restricts the choice of density parameter, since  $\Omega_i = \Omega_i(\lambda, \beta)$  during the scaling regime (see [16]). As the mass of the growing species is expected to vary by orders of magnitude we choose to identify the mass-growing species with neutrinos, fully considering the behavior of the neutrinos in the relativistic and non-relativistic regimes. As in Case II, we choose couplings of opposite sign, such that  $\beta_{\text{eff}}$  is driven towards zero during the matter dominated epoch.

We compare Case III with the growing-mass model of [47], who consider the dynamics of Attractor B with one coupled species. In our scenario, the field sits in the minimum of the effective potential; it becomes heavy due to the presence of multiple contributions from the fluids with couplings of opposite signs. This is not true in the growing-mass model.

As a final point we consider the evolution of the apparent equation of state, as discussed in [49]. For a system with multiple species of coupled fluids, the apparent equation of state of the dark energy sector as measured by an observer assuming an uncoupled system of fluids is given by

$$w_{\text{ap}} = \frac{w_\phi}{1 - x}, \quad (27)$$

where  $w_\phi \equiv \frac{p_\phi}{\rho_\phi}$  is the equation of state of the scalar field and

$$x \equiv \frac{1}{\rho_\phi} \sum_{i=1}^N \frac{\rho_i^{(0)}}{a^3} \left( 1 - \frac{\rho_i a^3}{\rho_i^{(0)}} \right) \quad (28)$$

$$= \frac{1}{\rho_\phi} \left( \frac{\rho_c^{(0)}}{a^3} - \rho_c \right). \quad (29)$$

It can be seen that in all of these models  $w_{\text{ap}}$  is rapidly varying and strongly negative, crossing through  $w_{\text{ap}} = -1$  close to  $z \sim 1$ . Note that in Case III the apparent equation of state becomes ill-defined, since  $x$  goes through unity. This is due to our choice of parameters.

### III. PERTURBATIONS

In the previous section we demonstrated that the background evolution of a cosmology with two fluids coupled to a single scalar field could be mimicked by a system with a single fluid coupled to a scalar field with an effective coupling given by eqn. (17). It is therefore impossible to distinguish between the two systems using probes of the cosmological background, such as measuring the expansion history. We have also seen that a system which comprises of multiple fluids with constant coupling strengths  $\beta_i$  may appear to be a single fluid with a time varying  $\beta$ , or indeed a system for which  $\beta = 0$  for at least some part during the matter dominated era. We now investigate the effect that these couplings have on the evolution of cosmological perturbations, and determine whether the degeneracy between the single fluid and the multi-fluid approach can be broken.

For each individual fluid, the equations governing the evolution of the density perturbations can be obtained from the perturbation of eqn. (5) and, at first order, are



given in the synchronous gauge by (see e.g. [50, 51])

$$\begin{aligned}\dot{\delta}_i &= 3 \left( H + \beta_i \dot{\phi} \right) \left( w_i - \frac{\delta p_i}{\delta \rho_i} \right) \delta_i - (1 + w_i) \left( \theta_i + \frac{\dot{h}}{2} \right) \\ &+ \beta_i (1 - 3w_i) \dot{\delta}\phi + \frac{d\beta_i}{d\phi} \dot{\phi} \delta\phi (1 - 3w_i)\end{aligned}\quad (30)$$

$$\begin{aligned}\dot{\theta}_i &= -H(1 - 3w_i)\theta_i - \frac{\dot{w}_i}{1 + w_i}\theta_i + \frac{\delta p_i/\delta \rho_i}{1 + w_i}k^2\delta_i \\ &+ \beta_i \frac{1 - 3w_i}{1 + w_i}k^2\delta\phi - \beta_i(1 - 3w_i)\dot{\phi}\theta_i - k^2\sigma_i,\end{aligned}\quad (31)$$

where for each species  $i$  we have defined:  $\delta_i = \delta\rho_i/\rho_i$  is the density contrast,  $\delta p_i$  is the pressure perturbation,  $h$  is a the metric perturbation,  $\theta_i$  is the gradient of the velocity field,  $\sigma$  is the shear stress and  $\delta\phi$  is the perturbation in the scalar field. For the HDM case, we use the full Boltzmann hierarchy to evaluate the density perturbations [44, 45].

The perturbed Klein-Gordon equation, governing the evolution of the scalar field perturbation  $\delta\phi$  is given by [50, 51]

$$\begin{aligned}\ddot{\delta\phi} + 2H\dot{\delta\phi} + \left( k^2 + a^2 \frac{d^2 V}{d\phi^2} \right) \delta\phi + \frac{1}{2}\dot{h}\dot{\phi} &= \\ -a^2 \sum_{i=1}^N \left[ \beta_i(\delta\rho_i - 3\delta p_i) + \frac{d\beta_i}{d\phi}\delta\phi(\rho_i - 3p_i) \right].\end{aligned}\quad (32)$$

The evolution of the density contrasts in the different cases are shown in Fig. 3, where we consider the limits of large and small scales. We now discuss both regimes separately.

### A. Small Scales

On small scales, the perturbed Klein Gordon equation can be approximated by

$$k^2\delta\phi + \frac{1}{2}\dot{h}\dot{\phi} = -a^2 \sum_{i=1}^N \beta_i \delta\rho_i, \quad (33)$$

where we have assumed that  $\beta_i$  is constant and  $w_i \sim 0$ . Using one of the perturbed Einstein equations [48]

$$\ddot{h} + H\dot{h} = -a^2 \sum_j \delta\rho_j \quad (34)$$

we can show that

$$\ddot{\delta}_i = - \left( H + \beta_i \dot{\phi} \right) \dot{\delta}_i + \frac{3}{2}H^2 \sum_{j=1}^N \Omega_j \delta_j \frac{G_{ij}^{\text{eff}}}{G_N} \quad (35)$$

where

$$G_{ij}^{\text{eff}} = G_N (1 + 2\beta_i \beta_j). \quad (36)$$

This equation has also been obtained in [51].

In Case I, where  $\beta_1\beta_2 > 0$ , the two species experience an additional attractive force between both similar and dissimilar particles, increasing the growth of the density perturbations. However in Case II,  $\beta_1$  and  $\beta_2$  have opposite signs, so whilst like particles feel an additional attractive force, two dissimilar particles experience a repulsive force between each other. This effect can be observed in the evolution of the density contrast in Fig. 3(a);  $\delta_i$  is enhanced in Case I whilst in Case II  $\delta_2$  is enhanced but  $\delta_1$  is suppressed (note that  $\delta_1$  becomes negative). For Case II, after horizon crossing, the dominant fluid (species 2) clusters at an enhanced rate due to the additional contribution to  $G^{\text{eff}}$ . Species 1 also feels an additional attractive force towards itself, but also experiences a repulsive force from species 2. As species 2 dominates the energy density, the bulk of the ordinary matter falls into the gravitational potential wells that it generates, whilst species 1 is repulsed from these overdensities.

However, note that during the period when the field is in it's minimum, the behavior of the combined fluid is identical to that of a single uncoupled species. It is only at late times, when the field evolves away from it's minimum due to the onset of dark energy domination, that the extra coupling force is felt, and the perturbations in the total fluid grow at an enhanced rate.

Case III is similar to Case II, except that the HDM undergoes freestreaming until it becomes non-relativistic, which suppresses the growth of the density contrast ( $\delta_1$ ).

### B. Large Scales

On superhorizon scales the evolution of  $\delta_i$  can be approximated by

$$\dot{\delta}_i = -\frac{\dot{h}}{2} + \beta_i \dot{\delta}\phi \quad (37)$$

for  $w_i = 0$ , which reduces to the usual expression for small values of coupling. The suppression of growth (prior to horizon crossing,  $z + 1 \geq 10^2$ ), seen in Fig. 3(b) for the highly coupled species, arises due to this additional coupling term, as the growth of  $\delta_i$  is modified by the term  $\beta_i \dot{\delta}\phi$ . In our models,  $\delta\phi$  is negative and we observe a suppression of  $\delta$ . However, once the mode enters the horizon, Eqn. (37) is no longer valid, the additional force between the particles mediated by dark energy can be felt and the growth of  $\delta_i$  is enhanced.

We point out that for all of the models considered in this paper, the range of the additional scalar force

$$\lambda \sim \frac{1}{m_\phi}, \text{ where } m_\phi^2 \equiv \frac{d^2 V}{d\phi^2} \quad (38)$$

is much greater than the horizon size and we do not therefore observe any effects due to the finite range of the force.

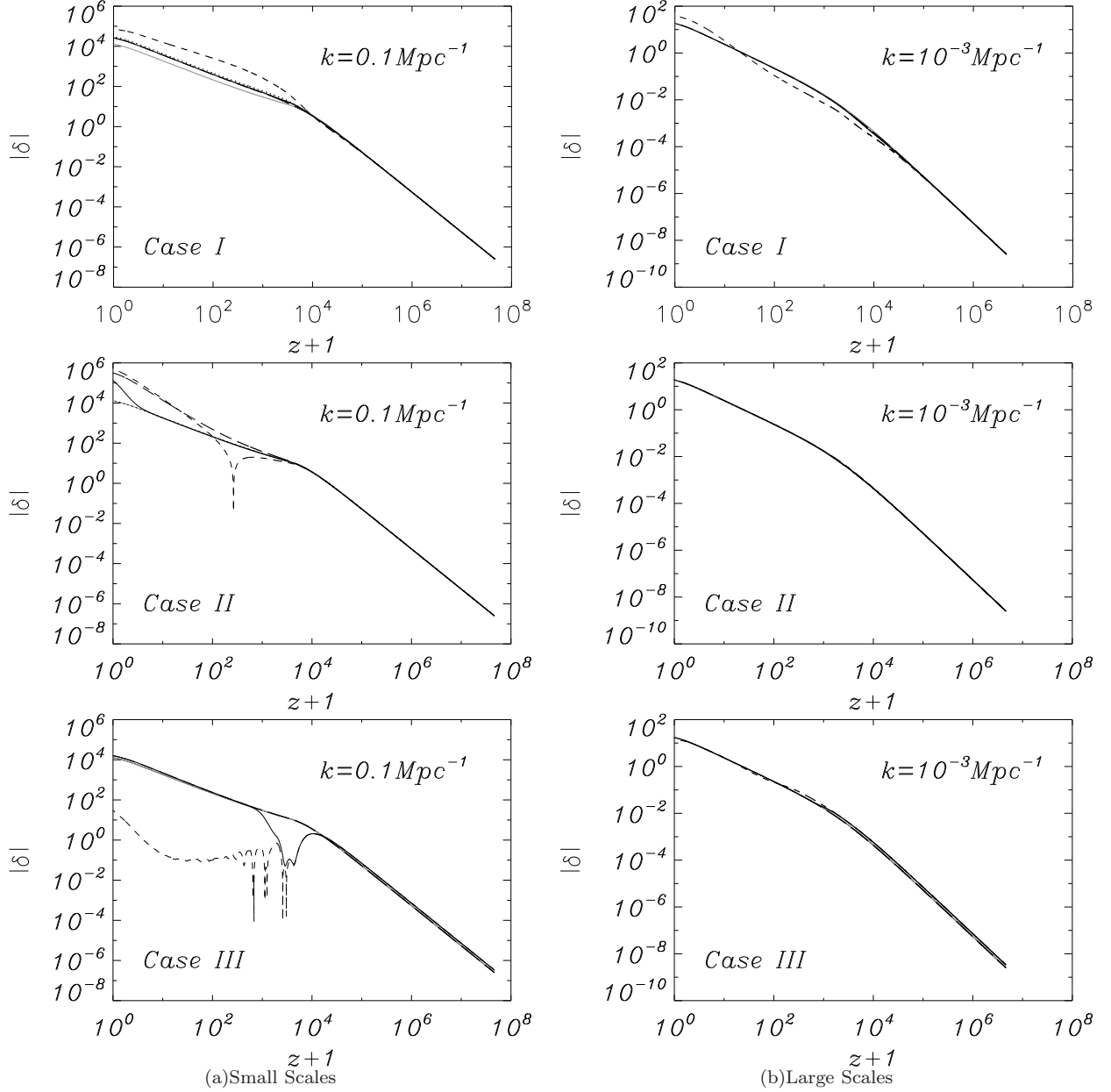


FIG. 3: Evolution of the density contrasts for the three cases on small and large scales. Thin solid line:  $\beta = 0$ . Short dashed line:  $\delta_1$ . Long dashed line:  $\delta_2$ . Thick solid line:  $\delta_c$ . Dotted line (Cases I and II only): equivalent single fluid with  $\beta = \beta_{\text{eff}}$ .

### C. Comparison to Equivalent Single Fluid

As for the background, we can consider the two species of matter to be a single fluid with

$$\delta\rho_c = \sum_{i=1}^N \delta\rho_i, \quad \delta_c = \frac{\delta\rho_c}{\rho_c}, \quad (39)$$

$$(\rho_c + p_c)\theta_c = \sum_{i=1}^N (\rho_i + p_i)\theta_i. \quad (40)$$

As explained in Section II, an observer studying the background evolution, who assumes only a single fluid dark matter sector, will infer that the coupling evolves in time,  $\beta_{\text{eff}} = \beta_{\text{eff}}(\phi)$ . With two dark matter species, an observer might detect a coupling of the form given in Eqn. (21).

However, it is apparent that we cannot re-write Eqns (30) and (32) into an equivalent single fluid form, due to the  $\frac{d\beta}{d\phi}$  term. Whilst for the single fluids  $\beta$  is purely a function of  $\phi$ , in the combined fluid  $\beta$  becomes a function of  $\phi$  and  $\rho_i$ . The term  $\delta\beta$  receives contributions from the variation of  $\phi$  and the variation of  $\delta\rho_i$ , which itself is a

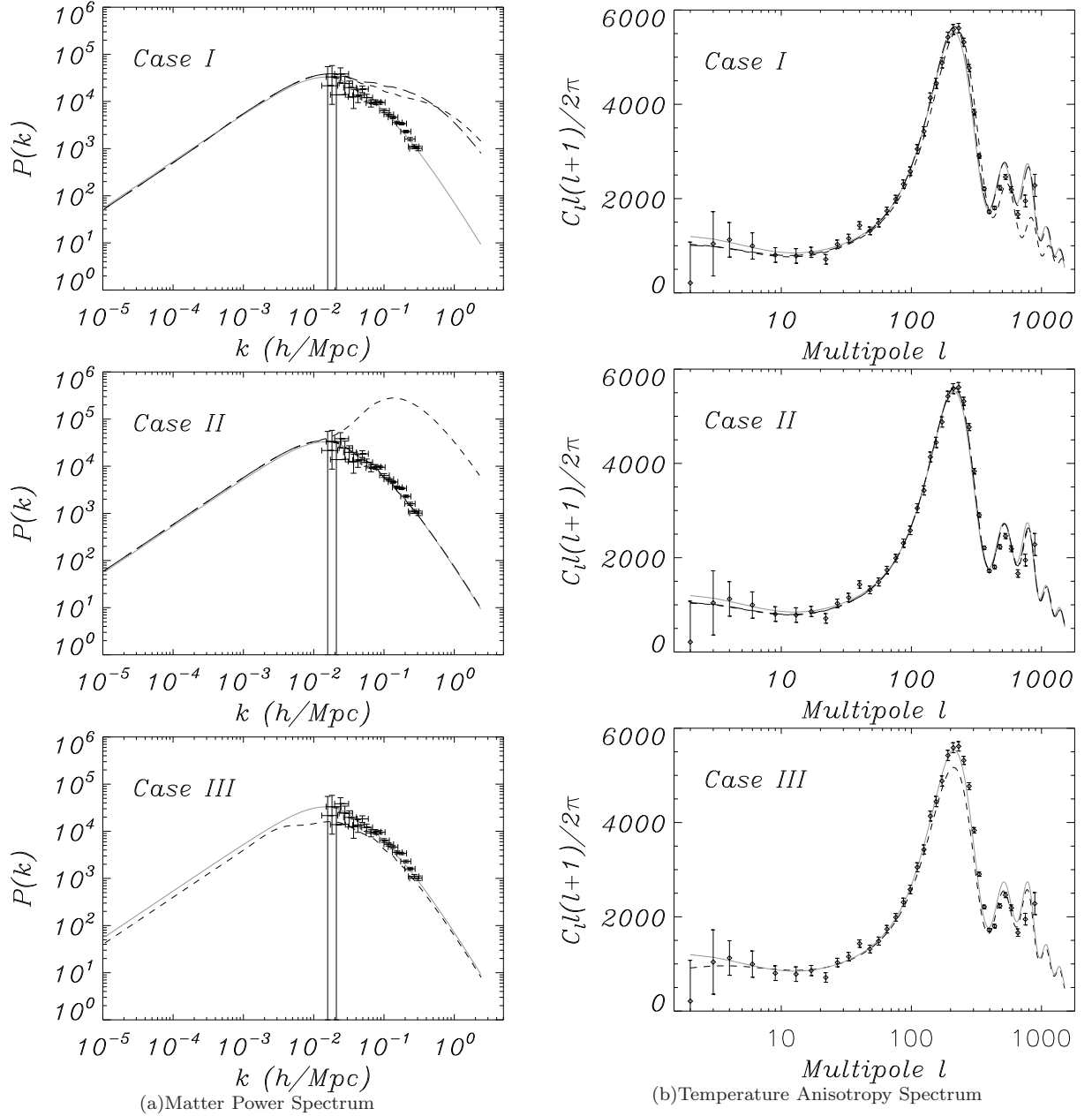


FIG. 4: CMB anisotropy spectra and matter power spectra for the three cases. Solid line:  $\beta = 0$ . Short dashed line: 2 coupled fluids. Long dashed line (Cases I and II only): single fluid with  $\beta = \beta_{\text{eff}}$ .

function of  $\phi$  and  $h$ . Hence, using  $\beta_{\text{eff}}(\phi)$  (inferred from background observations) to calculate the perturbation evolution would lead to incorrect predictions for  $\delta$ . For example, assuming a single fluid with an effective coupling leads to a different evolution of perturbations than if the observer had correctly identified two species.

In order to highlight this observational difference (allowing us to break the degeneracy), we calculate the evolution of perturbations for an equivalent single fluid model with field-varying coupling  $\beta_{\text{eff}}(\phi)$ . This is plotted in Fig. 3 for a direct comparison for Cases I and II.

(This effect is most apparent when we consider the matter power spectrum in the next section.) We also plot the case  $\beta = 0$  for comparison.

In Case II, when  $\beta_{\text{eff}} = 0$ , the density contrast of the combined fluid,  $\delta_c$ , mimics a single uncoupled fluid, which of course coincides with the equivalent single fluid (with  $\beta_{\text{eff}} = 0$ ) during this time.

For Case III, however, we do not compare the two fluid case with an equivalent single fluid. This is because  $\beta_{\text{eff}}$  is a function of both the pressure and energy density of the coupled species, one of which is highly relativistic



at early times. Although  $\beta_{\text{eff}}$  could be reconstructed as  $\beta_{\text{eff}}(\phi)$ , it would not take the simple analytic form given in Eqn. (21).

#### D. Observational Signatures

The differing behaviour of the perturbations for the multiple fluid and the single effective fluid leaves a detectable imprint on both the anisotropy spectrum and the matter power spectrum, as shown in Fig. 4. Once again, we compare the results for the multiple coupled fluids with the equivalent single coupled fluid with  $\beta = \beta_{\text{eff}}(\phi)$ . We remind the reader that the parameters are chosen such that the new effects of the interactions are emphasized.

For both Cases I and II, the matter power spectra are relatively unchanged on large scales, as the growth of density perturbations is weakly affected by the coupling (see Fig. 3(a)). On small scales, however, the enhanced growth of  $\delta_c$  is seen explicitly in the matter power spectra. The difference between multiple and single field fluids is apparent and breaks the degeneracy seen in the background solution.

In Case III, we see a suppression of power in the matter spectrum compared with the standard case. This is a consequence of the mass variation of the neutrinos, which are lighter in the past than in the standard case. They therefore undergo freestreaming for longer, which suppress the growth of density perturbations. This effect is partly compensated by the increased effective Newton's constant,  $G_{ij}^{\text{eff}}$ , experienced by the CDM particles, which would otherwise clump more than in the standard case.

Fig. 4(b) shows the effect of the coupled fluids on the temperature anisotropy spectrum. It has been shown previously that for a single coupled species of CDM, the coupling is constrained to  $|\beta| \lesssim 0.1$  [52], due to the large contribution from the coupling to the late-time Integrated Sachs–Wolfe (ISW) effect. For Cases I and II, however, we observe a reduction in the ISW effect, even though we have coupling strengths  $O(1)$ . This is because the effective coupling strength of the combined fluid in both Case I and Case II has been chosen to be  $O(0.1)$  at late times, to ensure that the ISW effect does not contribute too greatly on large scales. It should also be noted that, in a system with multiple coupled fluids, the fluid with the smallest  $\beta$  dominates the energy density of the coupled species at late times, as this species dilutes slower than species with larger couplings. In this scenario, therefore, we are not restricted by previous constraints on  $\beta$ .

For Case III, we can see that the contribution to the ISW from the coupling is enhanced relative to the height of the first acoustic peak.

An additional signature can be found in comparing the relative heights of the second and third peaks, which are significantly altered in Case I. This arises partly due to the change in relative energy densities at the time of last

scattering as seen in Fig. 1. For Cases II and III, the relative energy densities at this time remain unchanged as  $\beta_{\text{eff}} \rightarrow 0$  and the fluids mimic standard cosmology.

We can also see that there is a significant variation in the anisotropy spectrum and the matter power spectrum for the two coupled species of matter in comparison with the equivalent single species of matter. This difference therefore leaves a detectable signature, which allows differentiation between coupled fluids of single or multiple species.

#### IV. CONCLUSIONS

In this paper, we have considered the effect of new forces mediated by dark energy, considering a multi-component dark matter sector. From our study of the background, we have shown that multiple coupled fluids can mimic a single coupled species. In particular, multiple fluids with constant couplings (well motivated in particle physics) can behave like a single fluid with a time varying coupling. Additionally, the cosmological background can behave like a  $\Lambda$ CDM universe during the matter dominated epoch, for models in which the effective coupling vanishes.

We established that perturbations allow us to break this degeneracy between a single effective dark matter species and multiple fluids. Specifically, observers could distinguish between a single fluid with a time varying coupling  $\beta(\phi)$  and an effective fluid with an apparent time varying coupling.

Perturbation growth is affected on all scales by the couplings. On scales smaller than the horizon, particles feel a new force, mediated by the scalar field. Depending on the relative sign of the coupling, this force can be either attractive or repulsive. Depending on the coupling strength and relative densities, the growth of perturbations for a given species can be either enhanced or suppressed. We remark that the instabilities observed in [53, 54] are not present in the models considered here.

Compared to previous studies with a single fluid, CMB constraints on the strength of multiple couplings can be relaxed. We find that the system is not constrained to have  $\beta_i \lesssim 0.1$ . We expect stronger constraints to come from large scale structure surveys probing the matter power spectrum. Additionally, supernovae observations will constrain the evolution of the apparent equation of state, which can significantly deviate from  $w = -1$  and can even be  $w \leq -1$ . Observational constraints on these models should be considered in future work. Additionally, a study of non-linear perturbations on small scales should be undertaken, to identify further signatures of these interactions (such as in [43] and [55]). For example, the new interactions could modify the density profiles of dark haloes or induce a bias between baryons and dark matter. For a single coupled species, this was studied in [55], who conclude that cosmologies with dark-dark couplings are viable from an observational standpoint. It

would be interesting to generalise these findings to our models, but this is outside the scope of this paper.

### Acknowledgments

We are grateful to David Mota, Domenico Tocchini-Valentini and Christof Wetterich for useful discussions.

The authors acknowledge support from STFC.

- 
- [1] WMAP, D. N. Spergel *et al.*, *Astrophys. J. Suppl.* **170**, 377 (2007), astro-ph/0603449.
  - [2] U. Seljak, A. Slosar, and P. McDonald, *JCAP* **0610**, 014 (2006), astro-ph/0604335.
  - [3] M. Tegmark *et al.*, *Phys. Rev.* **D74**, 123507 (2006), astro-ph/0608632.
  - [4] S. M. Carroll, *Living Rev. Rel.* **4**, 1 (2001), astro-ph/0004075.
  - [5] C. Wetterich, *Nucl. Phys.* **B302**, 668 (1988).
  - [6] P. J. E. Peebles and B. Ratra, *Astrophys. J.* **325**, L17 (1988).
  - [7] C. Wetterich, *Astron. Astrophys.* **301**, 321 (1995), hep-th/9408025.
  - [8] I. Zlatev, L.-M. Wang, and P. J. Steinhardt, *Phys. Rev. Lett.* **82**, 896 (1999), astro-ph/9807002.
  - [9] P. Binetruy, *Phys. Rev.* **D60**, 063502 (1999), hep-ph/9810553.
  - [10] L. Amendola, *Phys. Rev.* **D62**, 043511 (2000), astro-ph/9908023.
  - [11] E. J. Copeland, N. J. Nunes, and F. Rosati, *Phys. Rev.* **D62**, 123503 (2000), hep-ph/0005222.
  - [12] E. J. Copeland, A. R. Liddle, and D. Wands, *Phys. Rev.* **D57**, 4686 (1998), gr-qc/9711068.
  - [13] P. Brax and J. Martin, *Phys. Lett.* **B468**, 40 (1999), astro-ph/9905040.
  - [14] P. Brax and J. Martin, *Phys. Rev.* **D61**, 103502 (2000), astro-ph/9912046.
  - [15] P. G. Ferreira and M. Joyce, *Phys. Rev.* **D58**, 023503 (1998), astro-ph/9711102.
  - [16] D. Tocchini-Valentini and L. Amendola, *Phys. Rev.* **D65**, 063508 (2002), astro-ph/0108143.
  - [17] R. Fardon, A. E. Nelson, and N. Weiner, *JCAP* **0410**, 005 (2004), astro-ph/0309800.
  - [18] J. Khoury and A. Weltman, *Phys. Rev.* **D69**, 044026 (2004), astro-ph/0309411.
  - [19] G. R. Farrar and P. J. E. Peebles, *Astrophys. J.* **604**, 1 (2004), astro-ph/0307316.
  - [20] P. Brax, C. van de Bruck, A.-C. Davis, J. Khoury, and A. Weltman, *Phys. Rev.* **D70**, 123518 (2004), astro-ph/0408415.
  - [21] A. W. Brookfield, C. van de Bruck, D. F. Mota, and D. Tocchini-Valentini, *Phys. Rev. Lett.* **96**, 061301 (2006), astro-ph/0503349.
  - [22] C. Armendariz-Picon, *JCAP* **0407**, 007 (2004), astro-ph/0405267.
  - [23] H. Wei and R.-G. Cai, *Phys. Rev.* **D73**, 083002 (2006), astro-ph/0603052.
  - [24] C. G. Boehmer and T. Harko, *Eur. Phys. J.* **C50**, 423 (2007), gr-qc/0701029.
  - [25] S. M. Carroll, V. Duvvuri, M. Trodden, and M. S. Turner, *Phys. Rev.* **D70**, 043528 (2004), astro-ph/0306438.
  - [26] S. M. Carroll *et al.*, *Phys. Rev.* **D71**, 063513 (2005), astro-ph/0410031.
  - [27] I. Navarro and K. Van Acoleyen, (2005), gr-qc/0511045.
  - [28] C. Deffayet, G. R. Dvali, and G. Gabadadze, *Phys. Rev.* **D65**, 044023 (2002), astro-ph/0105068.
  - [29] K. Freese and M. Lewis, *Phys. Lett.* **B540**, 1 (2002), astro-ph/0201229.
  - [30] D. A. Easson, *Int. J. Mod. Phys.* **A19**, 5343 (2004), astro-ph/0411209.
  - [31] S. Nojiri and S. D. Odintsov, *Phys. Rev.* **D68**, 123512 (2003), hep-th/0307288.
  - [32] T. Chiba, *Phys. Lett.* **B575**, 1 (2003), astro-ph/0307338.
  - [33] A. W. Brookfield, C. van de Bruck, and L. M. H. Hall, *Phys. Rev.* **D74**, 064028 (2006), hep-th/0608015.
  - [34] Y.-S. Song, W. Hu, and I. Sawicki, *Phys. Rev.* **D75**, 044004 (2007), astro-ph/0610532.
  - [35] R. Bean, D. Bernat, L. Pogosian, A. Silvestri, and M. Trodden, *Phys. Rev.* **D75**, 064020 (2007), astro-ph/0611321.
  - [36] S. Nojiri and S. D. Odintsov, (2007), arXiv:0707.1941 [hep-th].
  - [37] L. Amendola, D. Polarski, and S. Tsujikawa, *Phys. Rev. Lett.* **98**, 131302 (2007), astro-ph/0603703.
  - [38] T. Faulkner, M. Tegmark, E. F. Bunn, and Y. Mao, (2006), astro-ph/0612569.
  - [39] S. A. Appleby and R. A. Battye, (2007), arXiv:0705.3199 [astro-ph].
  - [40] I. Sawicki and W. Hu, *Phys. Rev.* **D75**, 127502 (2007), astro-ph/0702278.
  - [41] L. Amendola, R. Gannouji, D. Polarski, and S. Tsujikawa, *Phys. Rev.* **D75**, 083504 (2007), gr-qc/0612180.
  - [42] S. S. Gubser and P. J. E. Peebles, *Phys. Rev.* **D70**, 123510 (2004), hep-th/0402225.
  - [43] A. Nusser, S. S. Gubser, and P. J. E. Peebles, *Phys. Rev.* **D71**, 083505 (2005), astro-ph/0412586.
  - [44] A. W. Brookfield, C. van de Bruck, D. F. Mota, and D. Tocchini-Valentini, *Phys. Rev.* **D73**, 083515 (2006), astro-ph/0512367.
  - [45] K. Ichiki and Y.-Y. Keum, (2007), arXiv:0705.2134 [astro-ph].
  - [46] M. Kunz and D. Sapone, *Phys. Rev. Lett.* **98**, 121301 (2007), astro-ph/0612452.
  - [47] L. Amendola, M. Baldi, and C. Wetterich, (0600), arXiv:0706.3064 [astro-ph].
  - [48] C.-P. Ma and E. Bertschinger, *Astrophys. J.* **455**, 7 (1995), astro-ph/9506072.
  - [49] S. Das, P. S. Corasaniti, and J. Khoury, *Phys. Rev.* **D73**, 083509 (2006), astro-ph/0510628.
  - [50] C. S. Rhodes, C. van de Bruck, P. Brax, and A. C. Davis, *Phys. Rev.* **D68**, 083511 (2003), astro-ph/0306343.
  - [51] L. Amendola, *Phys. Rev.* **D69**, 103524 (2004), astro-

- ph/0311175.
- [52] L. Amendola and C. Quercellini, Phys. Rev. **D68**, 023514 (2003), astro-ph/0303228.
- [53] R. Bean, E. E. Flanagan, and M. Trodden, (2007), arXiv:0709.1124 [astro-ph].
- [54] R. Bean, E. E. Flanagan, and M. Trodden, (2007), arXiv:0709.1128 [astro-ph].
- [55] A. V. Maccio, C. Quercellini, R. Mainini, L. Amendola, and S. A. Bonometto, Phys. Rev. **D69**, 123516 (2004), astro-ph/0309671.

